Journal of Solid State Chemistry 183 (2010) 2183–2189

Contents lists available at ScienceDirect

Journal of Solid State Chemistry

journal homepage: www.elsevier.com/locate/jssc

Synthesis and structural characterization of $Al_4Si_2C_5$-homeotypic aluminum silicon oxycarbide, $(Al_{6-x}Si_x)(O_yC_{5-y})$ ($x\sim0.8$ and $y\sim1.6$)

Motoaki Kaga [a], Daisuke Urushihara [a], Tomoyuki Iwata [a], Keita Sugiura [a], Hiromi Nakano [b], Koichiro Fukuda [a,*]

[a] Department of Environmental and Materials Engineering, Nagoya Institute of Technology, Nagoya 466-8555, Japan
[b] Cooperative Research Facility Center, Toyohashi University of Technology, Toyohashi 441-8580, Japan

ARTICLE INFO

Article history:
Received 6 May 2010
Received in revised form
14 July 2010
Accepted 18 July 2010
Available online 24 July 2010

Keywords:
Aluminum silicon oxycarbide
Crystal structure
Rietveld method
Twin-related domain structure
$Al_4Si_2C_5$

ABSTRACT

We have prepared a new layered oxycarbide, $[Al_{5.25(5)}Si_{0.75(5)}][O_{1.60(7)}C_{3.40(7)}]$, by isothermal heating of $(Al_{4.4}Si_{0.6})(O_{1.0}C_{3.0})$ at 2273 K near the carbon–carbon monoxide buffer. The crystal structure was characterized using X-ray powder diffraction, transmission electron microscopy and energy dispersive X-ray spectroscopy (EDX). The title compound is trigonal with space group $R\bar{3}m$ (centrosymmetric), $Z=3$, and hexagonal cell dimensions $a=0.32464(2)$ nm, $c=4.00527(14)$ nm and $V=0.36556(3)$ nm^3. The atom ratios Al:Si were determined by EDX, and the initial structural model was derived by the direct methods. The final structural model showed the positional disordering of one of the three types of Al/Si sites. The reliability indices were $R_{wp}=4.45\%$ ($S=1.30$), $R_p=3.48\%$, $R_B=2.27\%$ and $R_F=1.25\%$. The crystal is composed of three types of domains with nearly the same fraction, one of which has the crystal structure of space group $R\bar{3}m$. The crystal structure of the remaining two domains, which are related by pseudo-symmetry inversion, is noncentrosymmetric with space group $R3m$.

1. Introduction

In the system Al–Si–O–C, the authors have discovered and structurally characterized two types of new aluminum silicon oxycarbides; $(Al_{18-x}Si_x)(O_yC_{14-y})$ ($x\sim1.2$ and $y\sim3.0$) [1] and $(Al_{5-x}Si_x)(O_yC_{4-y})$ ($x\sim0.6$ and $y\sim1.0$) [2]. Each of these crystals has been found to be made up of two domains, which are related by pseudo-symmetry inversion. The dimensions of twin domains have been within the coherence range of X-rays with the domain ratios being 0.5:0.5 for both compounds, hence the crystal structures have been successfully represented by the split-atom models. These compounds are characterized by the crystal structures consisting of two types of layers. One is an $[(Al,Si)_2(O,C)_2]$ double layer of $(Al,Si)(O,C)_4$ tetrahedra surrounded by two $[(Al,Si)(O,C)_2]$ single layers of $(Al,Si)(O,C)_4$ tetrahedra; these three layers form an $[(Al,Si)_4(O,C)_4]$ unit layer (A). The other is an $[(Al,Si)(O,C)_2]$ single layer (B) of $(Al,Si)(O,C)_4$ tetrahedra. The monoclinic structure of $(Al_{16.8}Si_{1.2})(O_{3.0}C_{11.0})$ (space group $C2/m$, $Z=1$) is build up of these two types of layers with the stacking sequence of $\langle ABA\rangle$. For the hexagonal lattice of $(Al_{4.4}Si_{0.6})(O_{1.0}C_{3.0})$ ($P6_3/mmc$, $Z=2$), the stacking sequence is $\langle ABAB\rangle$ and/or $\langle BABA\rangle$. Because the atomic configurations of $(Al_{16.8}Si_{1.2})(O_{3.0}C_{11.0})$ and $(Al_{4.4}Si_{0.6})(O_{1.0}C_{3.0})$ compare well with those of Al_8SiC_7 [3] and Al_4SiC_4 [4], respectively, they can be regarded as carbide solid solutions rather than oxycarbide compounds [1,2]. There are fifteen O/C sites in the unit cell for the former oxycarbide, 22% of which has been occupied by O atoms (O/(O+C)=0.22). On the other hand, the O atoms have occupied 25% of the sixteen O/C sites in the unit cell for the latter oxycarbide (O/(O+C)=0.25).

A series of ternary carbides in the Al_4C_3–SiC system can be represented by a general formula $Al_4C_3(SiC)_X$, where $X=1/2$ (Al_8SiC_7), 1 (Al_4SiC_4), 2 ($Al_4Si_2C_5$), 3 ($Al_4Si_3C_6$) and 4 ($Al_4Si_4C_7$) [1,3–7]. The crystal structures of Al_4SiC_4 and $Al_4Si_2C_5$ have been determined by single crystal X-ray diffraction method [4]. The structure of Al_4SiC_4 (space group $P6_3mc$, $Z=2$) is built up of alternately stacking $[(Al,Si)_4C_4]$ unit layer A and $[(Al,Si)C_2]$ single layer B with the sequence of $\langle BABA\rangle$. For the rhombohedral lattice of $Al_4Si_2C_5$ ($R\bar{3}m$, $Z=3$), the stacking sequence is $\langle BABBABBAB\rangle$. With $1/2\le X\le2$, the fraction of A layer (f_A) with respect to the B layer in the crystal structure steadily decreases with increasing X-value; the f_A- and X-values are well correlated by the equation $f_A=1/(1+X)$ [1]. The f_A-values as predicted by this relationship are 0.25 for $Al_4Si_3C_6$ ($X=3$) and 0.2 for $Al_4Si_4C_7$ ($X=4$). Assuming that these crystal structures were also made up of the two types of layers A and B, the minimum stacking sequences are $\langle BABB\rangle$ for $Al_4Si_3C_6$ and $\langle BBABB\rangle$ for $Al_4Si_4C_7$. These structures are comparable to those proposed by Oscroft et al. [5].

In the present study, we have succeeded in synthesizing a new aluminum silicon oxycarbide, which is homeotypic to $Al_4Si_2C_5$. We determined the initial structural model from XRPD data using direct methods and further modified it into a split-atom model, in

* Corresponding author.
E-mail address: fukuda.koichiro@nitech.ac.jp (K. Fukuda).

0022-4596/$ - see front matter © 2010 Elsevier Inc. All rights reserved.
doi:10.1016/j.jssc.2010.07.031

which one of the three types of Al/Si sites was positionally disordered. The crystal was most probably composed of three types of domains with ordered crystal structures.

2. Experimental

2.1. Synthesis

In a previous study, we prepared a powder specimen consisting of Al_4SiC_4-homeotypic aluminum silicon oxycarbide, $(Al_{4.4}Si_{0.6})(O_{1.0}C_{3.0})$ [2]. In the present study, we used this powder sample as the starting material, which was obtained by the following procedure. The reagent-grade chemicals of Al_4C_3 (98%, Mitsuwa Chemical Co., Ltd, Kanagawa, Japan) and SiC (99%, KCL Co., Ltd, Saitama, Japan) were mixed in molar ratios of Al_4C_3:SiC=1.5:1. The well-mixed chemicals were pressed into pellets (ϕ15 mm × 10 mm), loaded into an open carbon crucible, heated in a carbon resistance furnace at 2073 K for 1 h in inert gas atmosphere of Ar, followed by cooling to ambient temperature by cutting furnace power. The Ar gas that was flow in the furnace contained a very small amount of O_2 gas. Thus, the experimental oxygen partial pressure (P_{O_2}) was most probably near the carbon-carbon monoxide (CCO) buffer. The P_{O_2}-value at 2073 K was estimated to be 2.7×10^{-15} atm ($\log P_{O_2}=-14.57$) based on the CCO buffer (Fig. 1) [8]. The slightly sintered polycrystalline material was obtained, which exclusively consisted of the desired compound.

The starting material was pulverized into fine powder specimen and divided into two parts of 0.8 g each. One part of the sample was pressed into a pellet ($\phi10\times5$ mm), heated at 2273 K (200 K higher than the preparation temperature of the starting material) for 1 h, followed by cooling to ambient temperature by cutting furnace power. The cooling rate from 2273 to 1273 K was estimated to be 55 K/min. The reaction product was a sintered polycrystalline material (sample S-A). The other part was, without pressing into pellets, heated at 2273 K for 1 h, followed by cooling to ambient temperature by cutting furnace power (S-B). The sample as obtained was in a powdery state. The P_{O_2}-value at 2273 K was estimated to be 2.8×10^{-14} atm ($\log P_{O_2}=-13.56$) based on the CCO buffer (Fig. 1) [8].

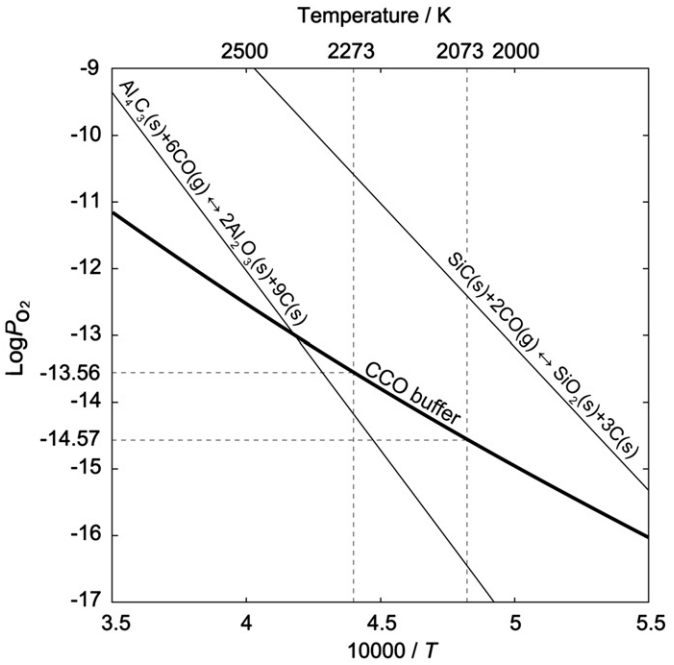

Fig. 1. Comparison of phase boundaries in the systems C–O, Al–O–C and Si–O–C as a function of temperature and oxygen partial pressure. The thick curve of carbon–carbon monoxide (CCO) buffer is from [8]. The curves of phase boundaries for $Al_4C_3(s)+6CO(g)\leftrightarrow2Al_2O_3(s)+9C(s)$ and $SiC(s)+2CO(g)\leftrightarrow SiO_2(s)+3C(s)$ are calculated using data from [20].

2.2. Characterization

The XRPD intensities for structural analysis were collected for S-B. A diffractometer (X'Pert PRO Alpha-1, PANalytical B.V., Almelo, the Netherlands), equipped with an incident-beam Ge(111) Johansson monochromator to obtain Cu$K\alpha_1$ radiation and a high-speed detector, was used in the Bragg–Brentano geometry. The X-ray generator was operated at 45 kV and 40 mA. An automatic divergence slit was used to keep a constant illuminated length of 5 mm on the specimen surface. Other experimental conditions were: continuous scan, experimental 2θ range from 5.0097° to 146.6878° (an accuracy in 2θ of $\pm0.0001°$), 8479 total data points and 5.5 h total experimental time. The entire experimental diffraction pattern was employed for the crystal-structure analysis. The structure data were standardized according to rules formulated by Parthé and Gelato [9] using the computer program STRUCTURE TIDY [10]. Structural parameters were refined by the Rietveld method using the computer program RIETAN-FP [11]. The quantitative X-ray analysis with correction for microabsorption according to Brindley's procedure [12] was implemented in the program. The crystal-structure models were visualized with the computer program VESTA [13]. The XRPD intensities for phase identification were collected for S-A. The experimental condition was: continuous scan, experimental 2θ range from 3.0167° to 64.9821°, 1855 total data points and 12.7 min total experimental time.

The sample S-B was also examined using a transmission electron microscope (JEM 2100F, JEOL ltd., Tokyo, Japan) operated at 200 kV and equipped with an energy dispersive X-ray analyzer (EDX; JED-2300, JEOL ltd., Tokyo, Japan). The powder particles were deposited with ethyl alcohol on a copper grid. Selected area electron diffraction (SAED) patterns and corresponding lattice images were obtained. A chemical analysis was made for ten crystal fragments to quantitatively determine the atom ratios Al:Si. The correction was made by the *ZAF* routines, which use fundamental factors to correct for the effects of atomic number (Z), absorption (A) and fluorescence (F).

3. Results and discussion

3.1. Crystal system, unit cell and chemical composition

The XRPD patterns indicated that considerable amount of starting material remained unreacted in the pelletized sample (S-A), while, in the pulverized sample (S-B), the starting material completely inverted to a new material together with a small amount of graphite. Thus, it is apparent that the temperature is not the only factor that converts the starting material into the new material; the interaction with gaseous phases would be indispensible for the conversion reaction.

The SAED pattern of the new compound in S-B was successfully indexed with a rhombohedral unit cell with hexagonal axes of $a\approx0.33$ and $c\approx4.0$ nm (Fig. 2). The corresponding lattice image strongly suggests that the crystal is characterized by a layered structure with the periodicity of about 4.0 nm along the c-axis. The EDX spectrum showed the existence of a small amount of O atoms within the crystal lattice (Fig. 3). The atom ratios Al:Si were determined to be 0.875(9):0.125(9), where the numbers in

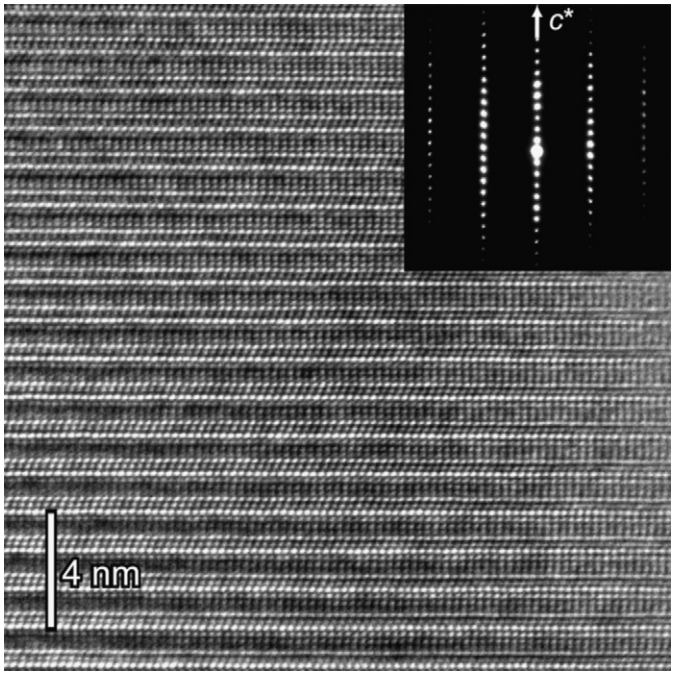

Fig. 2. Selected-area electron diffraction pattern and corresponding lattice image. Incident beam almost parallel to the hexagonal *a* axis.

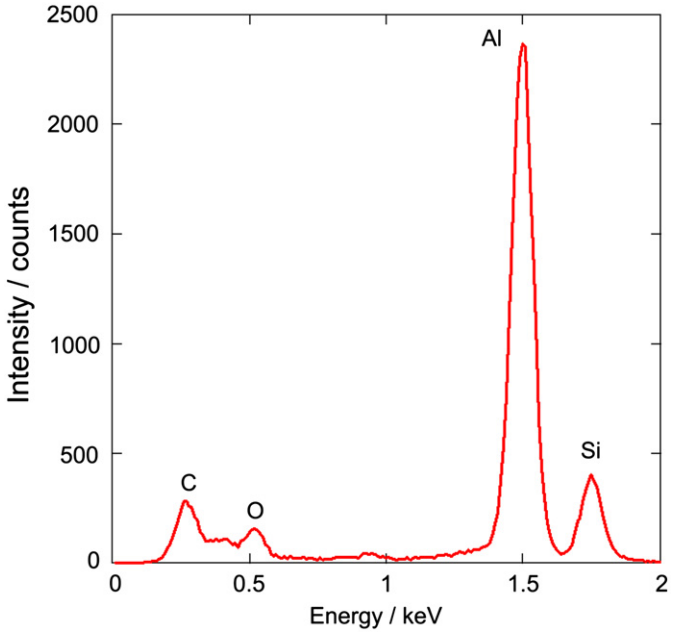

Fig. 3. Identification of the presence of Al, Si, O and C in the compound. EDX spectrum.

parentheses indicate standard deviations. It is noteworthy that the Al:Si ratios were, within error of measurement, identical to those of the starting material $(Al_{4.4}Si_{0.6})(O_{1.0}C_{3.0})$ (Al:Si=0.88:0.12). The intensity distributions of XRPD pattern as well as the cell dimensions were compatible with those of $Al_4Si_2C_5$ (V=0.36715 nm^3 and Z=3) [5]. Because the unit-cell content of this compound is [12Al 6Si 15C] (Al+Si=18), that of the new one must be [15.75Al 2.25Si 15(O+C)] (Al:Si=0.875:0.125, Al+Si=18), assuming that the O atoms exclusively occupy the C sites.

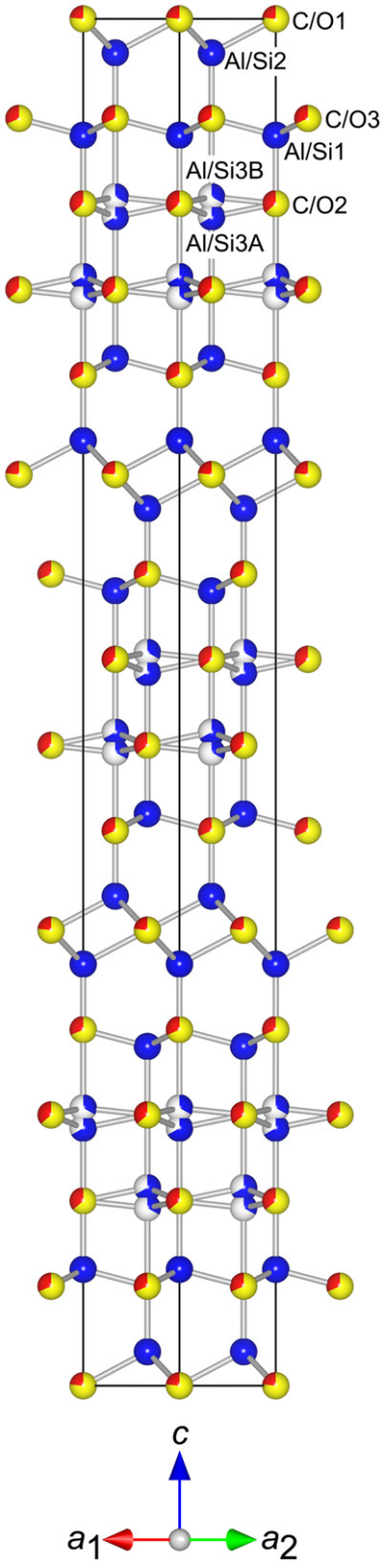

Fig. 4. Crystal structure of $(Al_{5.2}Si_{0.8})(O_{1.6}C_{3.4})$ viewed along [110]. Space group $R\bar{3}m$. All the atoms are expressed as solid spheres. Because the occupancies of Al/Si3A and Al/Si3B sites are less than unity, the Al/Si atoms occupying there are displayed as blue circle graphs for occupancies. Red and yellow bicolor balls are for oxygen (red) and carbon (yellow) sites. (For interpretation of the references to color in this figure legend, the reader is referred to the web version of this article.)

The XRPD pattern of S-B showed the presence of weak diffraction intensities peculiar to graphite. All of the other diffraction peaks belonging to the new material were successfully indexed with the rhombohedral unit cell. The hexagonal cell parameters and integrated intensities were refined by the Le Bail method [14], using the computer program RIETAN-FP. The refined cell dimensions were $a=0.324899(7)$ and $c=4.00512(9)$ nm. The integrated intensities were examined to confirm the presence or absence of reflections. There were no systematic absences for *hkil* reflections, implying that the possible space groups are $R3$, $R\bar{3}$, $R32$, $R3m$ and $R\bar{3}m$.

3.2. Structure refinement

Because the atomic scattering factors for Al and Si are almost the same and the oxygen concentration is relatively low, we used a unit-cell content with [18Al 15C] as input data for the search of a crystal-structure model. All of the possible space groups were tested using the EXPO2004 package [15] for crystal structure determination. The individual integrated intensities that were refined by the Le Bail method were used for the direct methods. A promising structural model with a minimum reliability index R_F of 28.3% was found with the space group $R\bar{3}m$ (centrosymmetric). There are six independent sites in the unit cell; three Al/Si sites (Al/Si1, Al/Si2 and Al/Si3) and two O/C sites (O/C2 and O/C3) are located at the Wyckoff position 6*c*, and one O/C site (O/C1) is located at 3*a*.

Structural parameters of all atoms were subsequently refined by the Rietveld method [16] using the computer program RIETAN-FP. The structural model of graphite was included in the refinement as the coexisting phase. A Legendre polynomial was fitted to background intensities with twelve adjustable parameters. The pseudo-Voigt function [17] was used to fit the peak profile. The preferred orientation parameter of March–Dollase function [18], $r_{\mathrm{Oxycarbide}}$, was refined to be 0.874(2) with the preferred-orientation vector [001], suggesting that the crystal grains were appreciably fractured along the cleavage planes parallel to (001). The Si and Al atoms were assumed to be randomly distributed over the same sites in the crystal structure, although there might be the site preference of these atoms. The occupancies (g) of O and C atoms in each O/C site were refined without any constraints. The isotropic displacement (B) parameters of the three O/C sites were constrained to be equal. Because g and corresponding B parameters were strongly correlated, they were refined alternately in successive least-squares cycles. The refinement however resulted in the relatively large B parameters for the Al/Si3 site ($B(\mathrm{Al/Si3})=2.28(3)\times10^{-2}$ nm^2) with the less satisfactory reliability (R) indices [19] of $R_{wp}=6.82\%$, $S\,(=R_{wp}/R_e)=1.90$, $R_p=5.25\%$, $R_B=3.60\%$ and $R_F=2.01\%$. These findings promoted us to build split-atom models for Al/Si3.

In the split-atom model, the Al/Si3 site was split into two independent crystallographic sites, Al/Si3A and Al/Si3B, with the same Wyckoff position 6*c*. The distribution of Al/Si atoms between each of these sites was determined by imposing the linear constrains of $g(\mathrm{Al/Si3A})+g(\mathrm{Al/Si3B})=1$. The parameters $B(\mathrm{Al/Si3A})$ and $B(\mathrm{Al/Si3B})$ were constrained to be equal. The final Rietveld refinement resulted in satisfactory R indices of $R_{wp}=4.45\%$, $S=1.30$, $R_p=3.48\%$, $R_B=2.27\%$ and $R_F=1.25\%$, indicating that the disordered arrangement of Al/Si3 site can be represented adequately with the split-atom model in Fig. 4. Observed, calculated, and difference XRPD patterns are plotted in Fig. 5. Crystal data are given in Table 1, and the final atomic positional and B parameters are given in Table 2. The separation distance between the Al/Si3A and Al/Si3B sites was 0.0594(2) nm. The g(Al/Si3A)- and g(Al/Si3B)-values converged very close to, respectively, 2/3 and 1/3. The chemical composition was found to be $Al_{5.25(5)}Si_{0.75(5)}O_{1.60(7)}C_{3.40(7)}$, with the chemical formula of $(Al_{5.2}Si_{0.8})(O_{1.6}C_{3.4})$ (space group $R\bar{3}m$, $Z=3$). The preferred orientation parameter of coexisting graphite, r_{Graphite}, was undetermined, hence the exact phase composition of S-B was uncertain. However, the concentration of graphite would be less than 3 mass % based on the probable relationship $r_{\mathrm{Graphite}} < r_{\mathrm{Oxycarbide}}$.

3.3. Structure description

In previous studies, each of the crystals $(Al_{16.8}Si_{1.2})(O_{3.0}C_{11.0})$ and $(Al_{4.4}Si_{0.6})(O_{1.0}C_{3.0})$ has been found to be made up of two domains,

Table 1
Crystal data for $(Al_{5.2}Si_{0.8})(O_{1.6}C_{3.4})$.

Chemical composition	$Al_{5.25(5)}Si_{0.75(5)}O_{1.60(7)}C_{3.40(7)}$
Space group	$R\bar{3}m$
a/nm	0.32464(2)
c/nm	4.00527(14)
V/nm^3	0.36556(3)
Z	3
D_x/Mgm^{-3}	3.123

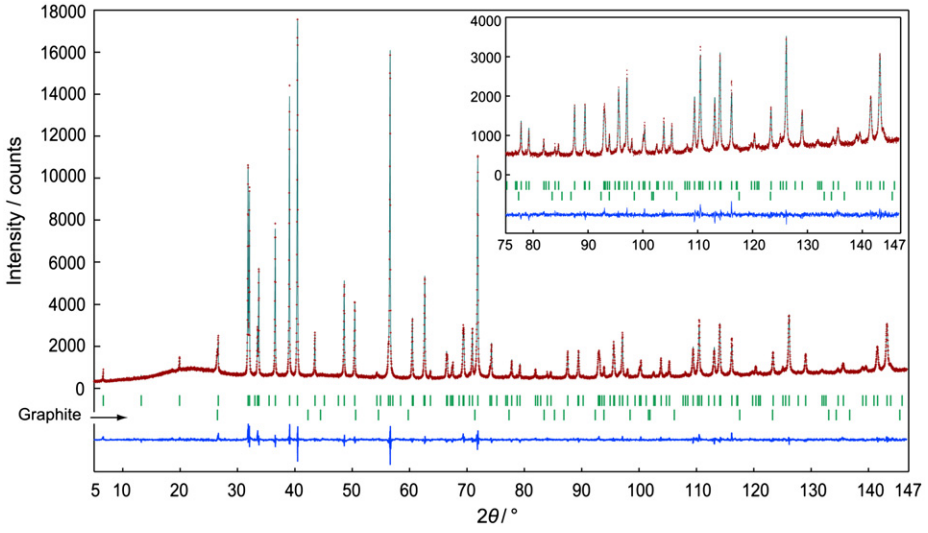

Fig. 5. Comparison of the observed diffraction pattern of $(Al_{5.2}Si_{0.8})(O_{1.6}C_{3.4})$ and graphite (symbol: +) with the corresponding calculated pattern (upper solid line). The difference curve is shown in the lower part of the diagram. Vertical bars indicate the positions of Bragg reflections.

which are related by pseudo-symmetry inversion [1,2]. One of the most plausible explanations to interpret the disordered crystal structure of $(Al_{5.2}Si_{0.8})(O_{1.6}C_{3.4})$ is to, in a similar manner, consider the structure to be a statistical average of several structural configurations. We have successfully extracted three types of ordered structural models I, II and III (Fig. 6) from the parent disordered structural model (Fig. 4). The crystal structure of the model I is centrosymmetric with the space group $R\bar{3}m$. This model is characterized by the absence of Al/Si3B site. On the other hand, both Al/Si3A and Al/Si3B sites are required for the models II and III, because their structures are noncentrosymmetric with the space group $R3m$. When the center of symmetry is removed from the space group $R\bar{3}m$, the resulting space group is $R3m$. The two structural configurations of II and III (Fig. 6) are therefore related by a pseudo-symmetry inversion. Thus, the crystal must be composed of three types of domains, two of which are related by inversion twinning. Because the site occupancies of the parent disordered model are nearly equal to 2/3 for Al/Si3A and 1/3 for Al/Si3B, the domain ratio should be almost 1/3:1/3:1/3. We actually observed using TEM interpenetrating domains (Fig. 7). The lattice fringes around the domain boundaries showed two types of translational misfits of approximately 0.3 and 0.5 nm along the common c-axis.

Table 2
Structural parameters for $(Al_{5.2}Si_{0.8})(O_{1.6}C_{3.4})$.[a]

Site	Wyckoff position	g	x	y	z	$100 \times B/nm^2$
Al/Si1	6*c*	1	0	0	0.08514(2)	0.89(6)
Al/Si2	6*c*	1	0	0	0.30847(2)	0.96(6)
Al/Si3A	6*c*	0.669(3)	0	0	0.18842(4)	0.91(6)
Al/Si3B	6*c*	0.331	0	0	0.20324(9)	0.91
O/C1	3*a*	1	0	0	0	1.53(9)
O/C2	6*c*	1	0	0	0.13520(5)	1.53
O/C3	6*c*	1	0	0	0.26053(6)	1.53

[a] Site occupancies: O/C1: 76.4(18)% C and 23.6(18)% O; O/C2: 63.5(12)% C and 36.5(12)% O; O/C3: 68.5(12)% C and 31.5(12)% O.

The crystal structure of $(Al_{5.2}Si_{0.8})(O_{1.6}C_{3.4})$ can be regarded as a layered structure, which consists of A-type $[(Al,Si)_4(O,C)_4]$ unit layers and B-type $[(Al,Si)(O,C)_2]$ single layers. The layer stacking sequences within the unit cells are $\langle BABBABBAB \rangle$ for model I, $\langle BBABBABBA \rangle$ for model II, and $\langle ABBABBABB \rangle$ for model III (Fig. 6). Thus, the layer stacking sequence of the former is, with respect to the latter two, displaced along the common c-axis by 0.27 nm, which corresponds to the B-type layer thickness. The layer stacking sequences of the models II and III are shifted mutually along the common c-axis by twice the B-type layer thickness of 0.54 nm. These magnitudes and directions of displacements are in agreement with those of the translational misfits between the interpenetrating domains (Fig. 7). The present domain boundaries are probably formed during crystal growth or phase transformations. The more detailed examination would be necessary to determine the origin of the domain structure.

In Table 3, only (Al,Si)–(O,C) bonds belonging to one of the two structural configurations II and III (space group $R3m$) are reported,

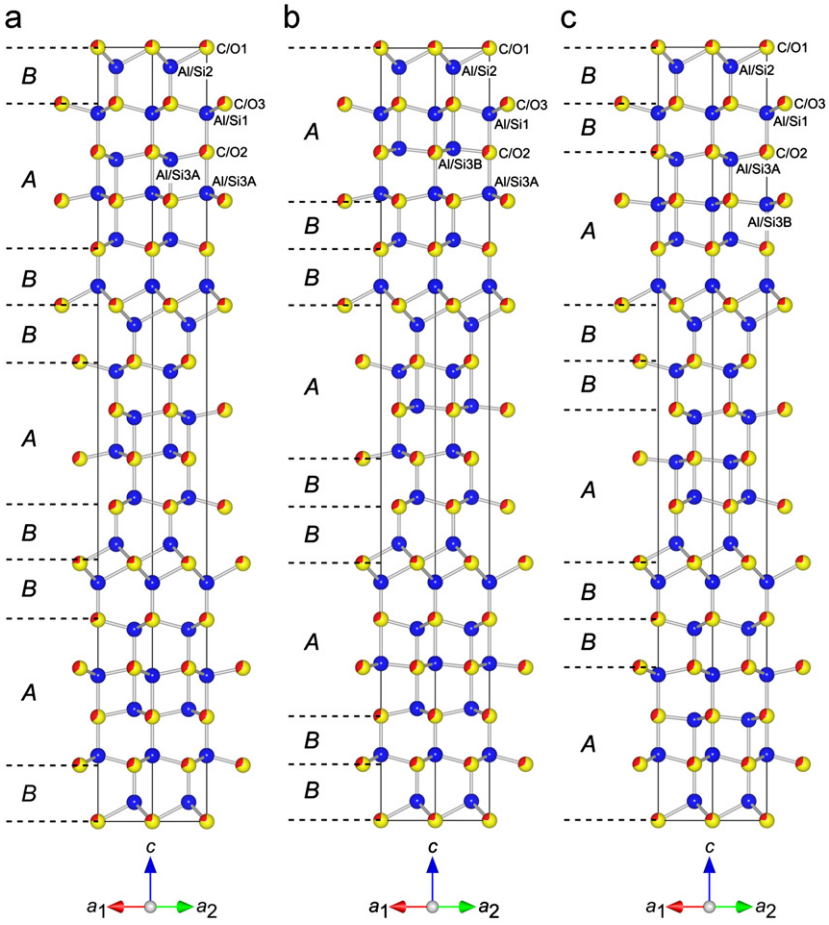

Fig. 6. Crystal structures of the three orientation states of $(Al_{5.2}Si_{0.8})(O_{1.6}C_{3.4})$ viewed along [110]. (a) Structural model I with the space group $R\bar{3}m$. Two structural configurations of models (b) II and (c) III with the space group $R3m$ are related by the pseudo-symmetry inversion. Individual crystal structures can be regarded as layered structures, which consist of A-type $[(Al,Si)_4(O,C)_4]$ unit layers and B-type $[(Al,Si)(O,C)_2]$ single layers.

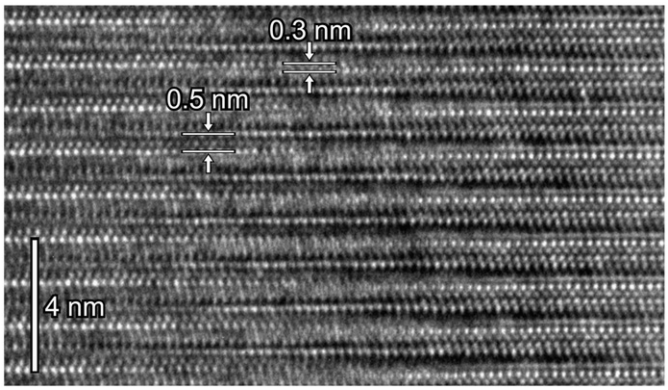

Fig. 7. Lattice image of mutually interpenetrating domains. Viewed along [100]. The fringes around the domain boundaries show translational misfits of approximately 0.3 and 0.5 nm along the common *c* direction.

Table 3
Interatomic distances (nm) in $(Al_{5.2}Si_{0.8})(O_{1.6}C_{3.4})$.

Al/Si1–O/C3	0.19383(6) × 3
Al/Si1–O/C2	0.2005(2)
⟨Al/Si1–O/C⟩	0.1955
Al/Si2–O/C3	0.1920(3)
Al/Si2–O/C1	0.21224(4) × 3
⟨Al/Si2–O/C⟩	0.2072
Al/Si3A–O/C2	0.19142(5) × 3
Al/Si3A–O/C2	0.2132(3)
⟨Al/Si3–O/C⟩	0.1969
Al/Si3B–O/C2	0.18854(5) × 3
Al/Si3B–O/C3	0.2295(4)
⟨Al/Si3–O/C⟩	0.1988

excluding possible bonds between atoms of different orientation states. With model I, the Al/Si3B–O/C bonds are missing because of the absence of Al/Si3B site. For all the three models, the Al and Si atoms are tetrahedrally coordinated by O and/or C atoms with the mean (Al,Si)–(O,C) distances of 0.200 nm, which are comparable to the mean (Al,Si)–(O,C) distances of $[(Al,Si)(O,C)_4]$ polyhedra in $(Al_{16.8}Si_{1.2})(O_{3.0}C_{11.0})$ (0.205 nm), $(Al_{4.4}Si_{0.6})(O_{1.0}C_{3.0})$ (0.202 nm) and $Al_4Si_2C_5$ (0.201 nm). There is a possibility of site preference of Al and Si in the Al/Si sites. Hence we tried to extract the information on site preference from the (Al,Si)–(O,C) distances; however the obtained results could not be regarded as significant. The mean interatomic distance as well as atomic configurations of $(Al_{5.2}Si_{0.8})(O_{1.6}C_{3.4})$ compare well with those of $Al_4Si_2C_5$ ($R\bar{3}m$). Thus, this oxycarbide is homeotypic to $Al_4Si_2C_5$ and regarded as, from a structural point of view, a carbide solid solution in which 32% C sites were occupied by O atoms rather than an oxycarbide compound. The general formula of the solid solution is expressed by $(Al_{6-x}Si_x)(O_yC_{5-y})$, where *x*- and *y*-values are, respectively, 0.8 and 1.6 for the sample. Further work is necessary to confirm the real existence of oxygen-free end member of $Al_4Si_2C_5$ ($x=1$ and $y=0$).

The conversion reaction from $(Al_{4.4}Si_{0.6})(O_{1.0}C_{3.0})$ to $(Al_{5.2}Si_{0.8})(O_{1.6}C_{3.4})$ is characterized by the increase in O/(O+C) ratio from 0.25 to 0.32 as well as the simultaneous formation of graphite. This implies that the Al_4C_3 and/or SiC components of the former are oxidized and the oxidizing CO gas is reduced to form graphite. Actually, the compound Al_4C_3 is unstable at temperatures 2073–2273 K near the CCO buffer (Fig. 1). It reacts with CO gas to form Al_2O_3 together with graphite as follows:

$$Al_4C_3(s)+6CO(g)\rightarrow 2Al_2O_3(s)+9C(s)$$

On the other hand, the compound SiC is stable between 2073 and 2273 K near the CCO buffer (Fig. 1). Although the thermodynamic behaviors of Al_4C_3 and SiC components in the crystal structures of aluminum silicon oxycarbides might be different from those of the individual compounds Al_4C_3 and SiC, the conversion reaction could be induced by the preferential oxidation of Al_4C_3 component of the starting material.

In the system Al–Si–O–C, the authors have discovered and structurally characterized the three types of new quaternary oxycarbides, $(Al_{16.8}Si_{1.2})(O_{3.0}C_{11.0})$ [1], $(Al_{4.4}Si_{0.6})(O_{1.0}C_{3.0})$ [2] and $(Al_{5.2}Si_{0.8})(O_{1.6}C_{3.4})$. These oxycarbides have the characteristics of the layered structures, hence the general formula is expressed by

$$(Al,Si)_{4l+m}(O,C)_{3l+m} \quad (1)$$

where *l* and *m* are, respectively, the numbers of *A*-type $[(Al,Si)_4(O,C)_4]$ unit layer and *B*-type $[(Al,Si)(O,C)_2]$ single layer of the minimum stacking sequence [2]. The (*l*, *m*) values are (2, 1) for $(Al_{16.8}Si_{1.2})(O_{3.0}C_{11.0})$, (1, 1) for $(Al_{4.4}Si_{0.6})(O_{1.0}C_{3.0})$ and (1, 2) for $(Al_{5.2}Si_{0.8})(O_{1.6}C_{3.4})$. In a similar manner, new types of oxycarbides are expected to form when O atoms were dissolved into the other ternary carbides than Al_8SiC_7, Al_4SiC_4 and $Al_4Si_2C_5$. Because the minimum stacking sequences are ⟨*BABB*⟩ for $Al_4Si_3C_6$ and ⟨*BBABB*⟩ for $Al_4Si_4C_7$, the corresponding (*l*, *m*) values of the general formula (1) are, respectively, (1, 3) and (1, 4).

4. Conclusion

In the Al–Si–O–C system, we have successfully synthesized a new $Al_4Si_2C_5$-homeotypic aluminum silicon oxycarbide, $(Al_{6-x}Si_x)(O_yC_{5-y})$ ($x\sim0.8$ and $y\sim1.6$). The crystal structure was satisfactorily represented by the split-atom model with the space group $R\bar{3}m$ (centrosymmetric). The crystal was composed of three types of domains with an almost 1/3:1/3:1/3 domain ratio. The dimension of twin domains was within the coherence range of X-rays, hence the crystal structure was successfully represented by the split-atom model. The new compound was, together with graphite, most probably formed by the preferential oxidation of Al_4C_3 component in $(Al_{4.4}Si_{0.6})(O_{1.0}C_{3.0})$.

Acknowledgment

Supported by a Grant-in-Aid for Scientific Research (No. 21360322) from the Japan Society for the Promotion of Science.

Appendix A. Supplementary material

Supplementary data associated with this article can be found in the online version at doi:10.1016/j.jssc.2010.07.031.

References

[1] T. Iwata, M. Kaga, H. Nakano, K. Fukuda, J. Solid State Chem. 182 (2009) 2252–2260.
[2] M. Kaga, T. Iwata, H. Nakano, K. Fukuda, J. Solid State Chem. 183 (2010) 636–642.
[3] B.L. Kidwell, L.L. Oden, R.A. McCune, J. Appl. Crystallogr. 17 (1984) 481–482.
[4] Z. Inoue, Y. Inomata, H. Tanaka, H. Kawabata, J. Mater. Sci. 15 (1980) 575–580.
[5] R.J. Oscroft, P. Korgul, D.P. Thompson, Br. Ceram. Proc. 42 (1989) 33–47.
[6] G.A. Jefeerey, V.Y. Wu, Acta Crystallogr. 20 (1966) 538–547.
[7] J. Schoennahl, B. Willer, M.J. Daire, Solid State Chem. 52 (1984) 163–173.
[8] I. S. Kulikov, Thermodynamics of Oxides, Metallurgiya, Moscow, USSR, 1986.
[9] E. Parthé, L.M. Gelato, Acta Crystallogr. A40 (1984) 169–183.
[10] L.M. Gelato, E. Parthé, J. Appl. Crystallogr. 20 (1987) 139–143.
[11] F. Izumi, K. Momma, Solid State Phenom. 130 (2007) 15–20.
[12] G.W. Brindley, Bull. Soc. Chim. Fr. (1949) D59–63.
[13] K. Momma, F. Izumi, J. Appl. Crystallogr. 41 (2008) 653–658.

[14] A. Le Bail, H. Duroy, J.L. Fourquet, Mater. Res. Bull. 23 (1988) 447–452.
[15] A. Altomare, M.C. Burla, M. Camalli, B. Carrozzini, G.L. Cascarano, C. Giacovazzo, A. Guagliardi, A.G.G. Moliterni, G. Polidori, R. Rizzi, J. Appl. Crystallogr. 32 (1999) 339–340.
[16] H.M. Rietveld, J. Appl. Crystallogr. 2 (1969) 65–71.
[17] H. Toraya, J. Appl. Crystallogr. 23 (1990) 485–491.
[18] W.A. Dollase, J. Appl. Crystallogr. 19 (1986) 267–272.
[19] R.A. Young, in: R.A. Young (Ed.), The Rietveld Method, Oxford University Press, Oxford, U.K1993, pp. 1–38.
[20] M.W. Chase Jr. (Ed.), NIST-JANAF Thermochemical Tables, J. Phys. Chem. Ref. Data Monograph No. 9, 4th ed., American Chemical Society and American Institute of Physics, Woodbury, NY, 1998.